NASA Technical Paper 3171

1992

Experimental Behavior of Graphite-Epoxy Y-Stiffened Specimens Loaded in Compression

P. Daniel Sydow
and Mark J. Shuart
Langley Research Center
Hampton, Virginia

NASA
National Aeronautics and Space Administration
Office of Management
Scientific and Technical Information Program

Abstract

An experimental investigation of the behavior of graphite-epoxy Y-stiffened specimens loaded in compression is presented. Experimental results are presented for element specimens with a single stiffener and for panel specimens with three stiffeners. Response and failure characteristics of the specimens are described. Effects of impact damage on structural response for both specimen configurations are also presented. Experimental results indicate that impact location may significantly affect the residual strength of the Y-stiffened specimens. The failure results indicate that the critical failure mode is buckling of the stiffener webs for Y-stiffened element specimens and buckling of the stiffener webs and the stiffener blades for the Y-stiffened panel specimens.

Introduction

Composite structures provide the aerospace engineer with unique opportunities in component design. An objective of NASA's Advanced Composites Technology (ACT) program is to investigate advanced design concepts for composite aircraft structures. Such advanced concepts include designs that exploit unique characteristics of composite structures and utilize cost-effective manufacturing procedures using advanced material systems or material forms. Stiffness tailoring is a well-known example of a unique characteristic of composite structures. Stiffness tailoring can be used to obtain structurally efficient composite components. An example of a potentially cost-effective manufacturing procedure for composite structures is pultrusion. Long prismatic structural elements may be pultruded to decrease hand lay-up and assembly efforts. An example of an advanced material system would be a low-cost damage-tolerant composite material system with high compression strength. Such a material would have many aircraft structures applications. The full potential for composite structures will be realized using effective advanced concepts.

Advanced concept composite structures that take advantage of both structural geometry and stiffness tailoring to achieve structural efficiency are being studied for application to primary aircraft structures such as wing cover panels. Previous design studies for metal structures have shown that a Y-stiffened panel configuration is highly structurally efficient (refs. 1 and 2). The Y-stiffener configuration combines the torsional rigidity of a closed-section design with the bending stiffness of a simple blade stiffener. A stiffness-tailored composite Y-stiffened panel is more structurally efficient than a similar metal panel, and the composite panel may also be fabricated cost effectively. The objectives of this paper are to describe the development of an optimized graphite-epoxy Y-stiffened cover panel concept, and to present the results of a study of the behavior of compression-loaded graphite-epoxy Y-stiffened specimens. Experimental results are presented for specimens with a single stiffener, referred to as Y-stiffened element specimens, and for panels with three stiffeners, referred to as Y-stiffened panel specimens. Response and failure characteristics of the specimens are described. Effects of impact damage on structural response for Y-stiffened element specimens and Y-stiffened panel specimens are also presented.

The authors would like to gratefully acknowledge the computer support given by Janice S. Myint in the reduction of the experimental data.

Concept Definition

The concept of a Y-stiffener configuration was first conceived in the late 1940's (refs. 1 and 2) and was referred to as the NACA Y-stiffener. This stiffener is shown in figure 1(a). Design requirements for metal stiffeners included a high column buckling load and high local buckling loads. The metal NACA Y-stiffener has a stiffener cap to achieve the required column buckling load and sufficiently thick webs to suppress local buckling. Optimized configurations were determined using a graphical technique that plotted a weight index as a function of the average stress resultant for the panel (ref. 1).

A composite Y-stiffener is shown in figure 1(b). The optimized design for this stiffener was obtained using the Panel Analysis and Sizing Code (PASCO) (ref. 3). The optimized panel was designed to carry a combined loading condition of $N_x = 14\,660$ lb/in., $N_y = 733$ lb/in.,r and $N_{xy} = 1367$ lb/in., where N_x, N_y, and N_{xy} are in-plane stress resultants. This loading condition was selected as representative of a high compression-dominated loading for the cover panel of a high-aspect-ratio subsonic commercial transport wing. The design variables used in the structural optimization of this panel were stiffener planform dimensions and thicknesses. Lamina properties used for the structural optimization are given in table 1. The optimized stiffener from the combined-load panel was used as the stiffener for the present study. The stacking sequences for this composite stiffener are shown in figure 2. The cap for the metal NACA Y-stiffener is not required for the optimized composite stiffener because stiffness and load-carrying requirements can be satisfied without a stiffener cap. Absence of the stiffener cap for the

composite stiffener is an example of how stiffness tailoring for composite structures can simplify designs.

Table I. Properties for IM7/8551-7A Used for Structural Optimization

Longitudinal Young's modulus, E_{11}, Msi	20.9
Transverse Young's modulus, E_{22}, Msi	1.5
Shear modulus, G_{12}, Msi	0.72
Poisson's ratio, ν_{12}	0.33
Nominal ply thickness, in.	0.0055

Specimens, Apparatus, and Tests

Composite Y-stiffened specimens were fabricated from a commercially available, advanced damage-tolerant material system, Hercules IM7/8551-7A graphite-epoxy preimpregnated tape. The tapes were laid to form 24-ply-thick flat laminates for the specimen skins with laminate stacking sequence $[\pm 45/0/\mp 45/0/\pm 45/0/\mp 45/90]_S$. Tapes were also laid on the manufacturing tool as shown in figure 2 to form halves for the specimen Y-stiffeners. The flanges and webs of the stiffeners are 16-ply-thick laminates having a $[\pm 45/90/\mp 45/90/\pm 45]_S$ stacking sequence. The blade region for the stiffener halves of the stiffeners is a 23-ply-thick laminate having a $[+45/0_4/-45/0_3/+45/\overline{0}_3]_S$ stacking sequence. Some of the $\pm 45°$ plies from the flanges and webs are continuous through the blade. All laminates were cured in an autoclave using the manufacturer's recommended procedures. Following cure, the laminates were ultrasonically C-scanned to establish specimen quality. The stiffener halves were bonded together after curing to form the Y-stiffener, and the Y-stiffeners were subsequently bonded to the specimen skins. Hysol EA 934 adhesive was used for all bonding.

Typical specimens used in this study are shown in figure 3. The Y-stiffened element specimen consists of a 20-in-long by 5.78-in-wide skin and a single stiffener, as shown in figure 3(a). The Y-stiffened panel specimen consists of a 20-in-long by 17.34-in-wide skin and three evenly spaced stiffeners, as shown in figure 3(b). The specimen ends were secured in a potting material to introduce load into the structure. The specimen ends were inserted approximately 1 in. into the potting material, making the effective specimen test section approximately 18 in. long. The loaded ends of the specimens were machined flat and parallel to permit uniform compressive end-shortening. The unstiffened side of the skin of each specimen was painted white to increase surface reflectivity so that a moiré fringe technique could be used to detect and monitor any out-of-plane deformations during testing. Three element specimens and two panel specimens were fabricated. Stiffened element specimens were designated NY1 through NY3, and stiffened panel specimens were designated NYP1 and NYP2. The specimens were loaded quasi-statically in uniform axial compression using a 300-kip-capacity hydraulic testing machine. The unloaded edges of the skins were simply supported to prevent the specimens from buckling as a column. All specimens were loaded to failure.

A procedure described in reference 4 for impacting graphite-epoxy components was used in the current investigation. Aluminum spheres 0.50 in. in diameter were used as impact projectiles. These spheres are propelled by a compressed-air gun equipped with an electronic detector to measure projectile speed. All projectile speeds in this study were approximately 550 ft/sec, which corresponds to an impact energy of approximately 27.5 ft-lb. A schematic of the air gun and a description of its operation are given in reference 4.

Impact sites for specimens in this study are shown in figure 4. Two of the Y-stiffened elements, NY2 and NY3, were subjected to impact damage prior to testing. Specimen NY2 was impacted at two locations on the unstiffened side of the skin opposite the attachment flanges. The first impact was at one-quarter of the test section length, and the second impact was at the midpoint of the test section length, as shown in figure 4(a). Specimen NY3 was impacted once at the midpoint of the test section length on the blade in the vicinity of the transition region of the web and the blade, also shown in figure 4(a).

One of the Y-stiffened panels, NYP2, was subjected to impact damage. NYP2 was impacted at two locations on the unstiffened side of the skin opposite the attachment flanges of the center stiffener prior to testing. The first impact was at one-quarter of the test section length, and the second impact was at the midpoint of the test section length as shown in figure 4(b). This panel was loaded to a 0.006 in/in. strain level and then unloaded. NYP2 was then impacted at the midpoint of the central blade in the vicinity of the transition region of the web and the blade and loaded to failure.

The specimens were instrumented with electrical resistance strain gages applied to the flanges, webs, and blades of the Y-stiffened elements, and to the skin, webs, and blades of the Y-stiffened panels. Direct-current differential transformers were used to measure specimen end-shortening and out-of-plane displacements. Electrical signals from the instrumentation and the corresponding applied loads were

electronically recorded at regular time intervals during the test.

Results and Discussion

Y-Stiffened Element Specimens

Normalized load/end-shortening results are presented in figure 5 for the three Y-stiffened element specimens. The applied load is normalized by the membrane stiffness, and the end-shortening is normalized by the specimen length. This normalized end-shortening is a measure of the specimen's global strain. The solid circles indicate specimen failure. These load/end-shortening results appear nearly linear up to a global strain of approximately 0.005 in/in. The slight deviation from a linear response may be attributed to initial imperfections. The first specimen, NY1, failed at 93.0 kips and a global strain of 0.0096 in/in. The second specimen, NY2, which was impacted on the unstiffened side of the skin opposite the attachment flanges, failed at 74.3 kips and a global strain of 0.0085 in/in. The third specimen, NY3, which was impacted near the web-blade interface, failed at 50.1 kips and a global strain of 0.0051 in/in. The failure loads for damaged specimens NY2 and NY3 are 20 percent lower and 46 percent lower, respectively, than the failure load for the undamaged specimen NY1. The effects of impact damage on element specimen failure are discussed below.

The strain results for the Y-stiffened element specimens are shown in figures 6–8. These strain results were obtained from gages on each specimen, as shown in figures 6(a), 7(a), and 8(a). Strain results for the undamaged specimen NY1 are presented in figure 6. The axial strain from back-to-back strain gages on the skin-flange region is shown in figure 6(b) as a function of the applied load. The symbols represent specimen failure. This slightly nonlinear strain behavior is similar to the load/end-shortening behavior. No strain reversal is observed. These results indicate that no bending or buckling occurs in this region during the test. The axial (parallel to the load direction) and the transverse (perpendicular to the load direction) strains in the webs are shown in figure 6(c) as a function of the applied load. Axial strains in each specimen web are shown for location B1, and these strains are always compressive. Transverse strains in each web are shown for location B2, and these strains are always tensile. The axial strain results for the webs are similar to the axial strain results for the skin-flange region (fig. 6(b)). The transverse strain results for the webs show strain reversal, indicating that the webs buckle prior to failure. Axial strain results for the blade are presented in figure 6(d). These results are similar to the axial strain results for the skin-flange region and the web.

Strain results for the impact-damaged element specimen NY2 are presented in figure 7. The axial strain from back-to-back strain gages located on the skin-flange region is shown in figure 7(b) as a function of applied load. The symbols represent specimen failure. The slight differences in the back-to-back strains for a given load level indicate that local bending or buckling occurred. The axial and transverse strains in the webs are shown in figure 7(c) as a function of the applied load. The compressive axial strain behavior is linear to failure for one web and nonlinear for the other web. The nonlinear behavior indicates bending of this web that is adjacent to the impact-damaged region. The slight strain reversal observed for the tensile transverse strain results suggests that the webs buckle just prior to failure. The web transverse strain behavior for the damaged specimen is similar to the web transverse strain behavior for the undamaged specimen NY1, but the failure strain for the damaged specimen is less than the failure strain for the undamaged specimen. Axial strain results for the blade of specimen NY2 are presented in figure 7(d). These results are similar to the axial strain results for the skin-flange region of this specimen. All failure strains in figure 7 for damaged specimen NY2 are less than the corresponding failure strains in figure 6 for undamaged specimen NY1. However, the global failure strain for damaged specimen NY2 is greater than 0.0085 in/in., indicating good residual strength in spite of impact damage at the skin-flange region. Good residual strength is defined for this study as global failure strains being greater than or equal to 0.006 in/in. in spite of the presence of impact damage.

Strain results for the impact-damaged element specimen NY3 are presented in figure 8. The axial strain from back-to-back strain gages on the skin-flange region is shown in figure 8(b) as a function of applied load. These strain results are approximately linear to failure, and no strain reversal is observed. The axial and transverse strains in the webs are shown in figure 8(c) as a function of the applied load. The compressive axial strain behavior is linear to failure for one web and nonlinear for the other web. The nonlinear behavior indicates bending of the web adjacent to the impact-damaged region. The strain reversal observed for the tensile transverse strain results indicates that these webs buckled prior to failure. The web axial and transverse strain behavior for this damaged specimen NY3 is similar to the web axial and transverse strain behavior for the damaged specimen NY2. Axial strain results for the

blade of specimen NY3 are presented in figure 8(d). The strain reversal observed for these axial strains indicates that the blade buckled prior to failure. All failure strains in figure 8 for specimen NY3 are less than the corresponding failure strains in figure 7 for specimen NY2. These failure strain data and the failure load and global failure strain results for specimens NY2 and NY3 indicate that, for the same impact energy, impact damage at the blade-web interface degrades the undamaged structural response of this Y-stiffener configuration more than impact damage at the skin-flange region. The global failure strain for damaged specimen NY3 is approximately 0.005 in/in., indicating marginal residual strength to an impact at the blade-web interface.

The dominant response that initiates failure of these Y-stiffened element specimens is web buckling. Web buckling is a significant design consideration for Y-stiffeners, since the webs support the blade. The blade is the primary load-carrying section for this configuration. All three specimens have web strain data that indicate web buckling prior to failure. No buckling was observed from the moiré fringe pattern during the element specimen tests, indicating that the specimen skin does not buckle. Blade buckling, as indicated by strain gage reversal, only occurs for the specimen impacted at the blade-web intersection. Web buckling may also contribute to the debonding of the adhesively bonded halves of these Y-stiffener blades. A typical failed element specimen and a close-up of the failure region are shown in figure 9.

Y-Stiffened Panel Specimens

Normalized load/end-shortening results are presented in figure 10 for the two Y-stiffened panel specimens. The applied load is normalized by the membrane stiffness, and the end shortening is normalized by the specimen length. The solid circles indicate failure of the specimen, and the open circle indicates termination of the test prior to failure. All results appear nearly linear up to a global strain of approximately 0.005 in/in. The slight deviation from a linear response may be attributed to initial imperfections. Photographs of moiré fringe patterns just prior to specimen failure are shown in figure 11. The results for the first specimen, NYP1, in figure 11(a) indicate that the skin's buckling mode shape is characterized by five half-waves along the length and two half-waves across the width between the stiffeners of the specimen. Specimen NYP1 failed at 285.2 kips and a global strain level of 0.0078 in/in. The test of the second test specimen, NYP2, was conducted in two phases. First, NYP2 was impacted at two locations on the unstiffened side of the skin opposite the attachment flanges of the center stiffener, in a similar manner as Y-stiffened element NY2 (see fig. 4(b)). The panel was then loaded to a 0.006 in/in. global strain level to simulate the ultimate compressive strain level for a wing cover panel. The panel did not buckle and did not fail when loaded to a global strain level of 0.006 in/in. In the next phase of the test, NYP2 was impacted once more. The impact site was at the midpoint of the test section length and on the central blade in the vicinity of the transition region of the web and the blade (see fig. 4(b)). This location was determined to be the critical impact site from the previous tests of Y-stiffened element specimens. The panel was then loaded until the center stiffener failed at 137.1 kips at a global strain of 0.0045 in/in. The results for specimen NYP2 in figure 11(b) show that the skin's buckling mode shape is characterized by a single half-wave along the length and a single half-wave across the width. This mode shape occurs after separation of the center stiffener from the skin but prior to separation of the skin from the remaining stiffeners. The specimen NYP2 fails when the skin debonds from the outer stiffeners at 137.2 kips and a global strain of 0.0057 in/in. The maximum loading for the impact-damaged panel was 48 percent less than the maximum loading for the undamaged panel. The effects of damage on panel specimen failure are discussed below.

The strain results for the Y-stiffened panel specimens are shown in figures 12 and 13. These strain results were obtained from gages on each specimen, as shown in figures 12(a) and 13(a). Strain results for the undamaged specimen NYP1 are presented in figure 12. The axial strain from back-to-back strain gages on the skin between stiffeners is shown in figure 12(b) as a function of the applied load. The symbols represent specimen failure. This slightly nonlinear strain behavior is similar to the load/end-shortening behavior. No strain reversal is observed. These results indicate that slight bending occurs in this region just prior to failure. The axial and transverse strains in the webs are shown in figure 12(c) as a function of the applied load. Axial strains in each specimen web are shown for location B1, and these strains are always compressive like the web axial strains for the stiffened element specimens. Transverse strains in each web are shown for location B2, and these strains are always tensile like the web transverse strains for the stiffened element specimens. The axial strain results for the webs are similar to the axial strain results for the skin (fig. 12(b)). The transverse strain results for the webs show strain reversal, which indicates that the webs buckled prior to failure. Axial strain results for the blade are presented in figure 12(d). These results

show strain reversal, which indicates buckling of the blade.

Strain results for the impact-damaged panel specimen NYP2 are presented in figure 13. These results correspond to the second phase of the test, in which the panel was loaded to failure. All results for the first phase of the test are linear and have the same slope as the initial slope for the corresponding strain behavior for the second phase of the test. The axial strain for the second phase of the test from back-to-back strain gages on the skin between stiffeners is shown in figure 13(b) as a function of applied load. These strain results show only the slightest indication of local bending in the skin. The axial and transverse strains in the webs are shown in figure 13(c) as a function of the applied load. The compressive axial strain results indicate that buckling of both webs occurred. The strain reversal observed for the tensile transverse strain results at a strain level of 0.005 in/in. indicates that these webs buckled prior to failure. Axial strain results for the blade of specimen NYP2 are presented in figure 13(d). The strain reversal observed for these axial strains indicates that the blade of the impact-damaged specimen buckles at a much lower load level than the blade of the undamaged specimen as a result of the impact damage in the blade near the blade-web interface. The significant difference in the strains of the back-to-back strain gages suggests that buckling of the blade may have caused a midplane interlaminar shear failure of the blade. All failure strains in figure 13 for specimen NYP2 are less than the corresponding failure strains in figure 12 for specimen NYP1. The global failure strain for damaged specimen NYP2 is approximately 0.0057 in/in., indicating marginal residual strength of this panel subjected to a combined impact at the skin-flange region and at the blade-web interface.

Photographs of the failed panel specimens NYP1 and NYP2 are shown in figures 14 and 15, respectively. Both specimens have failures in the test section of the panel. The damage as a result of failure appears more severe for specimen NYP1 when compared with the damage as a result of failure for specimen NYP2. This difference is due to the much higher failure load of specimen NYP1. The strain results for these panel specimens indicate that both buckling of the web and buckling of the blade occur. These results do not conclusively indicate that one region buckles before the other. The results do indicate that web buckling and blade buckling are important design considerations for Y-stiffened panels.

Concluding Remarks

This paper describes an experimental investigation of the behavior of graphite-epoxy Y-stiffened specimens loaded in compression. Response and failure characteristics are presented for specimens with a single stiffener, referred to as Y-stiffened element specimens, and for specimens with three stiffeners, referred to as Y-stiffened panel specimens. Effects of impact damage on structural response for both specimen configurations are discussed.

Impact location may significantly affect the residual strength of the Y-stiffened specimens. The element specimen impacted on the unstiffened side of the skin and opposite the stiffener flanges had a global failure strain greater than 0.0085 in/in., indicating good residual strength for this specimen impacted at the skin-flange region. The element specimen impacted near the blade-web interface had a global failure strain of approximately 0.005 in/in., indicating marginal residual strength. The failure results for the damaged element specimens show that, for the same impact energy, an impact at the blade-web interface degrades the undamaged structural response more than an impact at the skin-flange region. The dominant mechanism that initiates failure for all the Y-stiffened element specimens is web buckling. The damaged panel specimen was first impacted on the unstiffened side of the skin (opposite the stiffener flanges of the center stiffener) and loaded to a global strain level of 0.006 in/in. The specimen was next impacted near the blade-web interface of the center stiffener. This resulted in a global failure strain of 0.0057 in/in., indicating marginal residual strength. The dominant mechanism that initiates failure for all the Y-stiffened panel specimens is combined web and blade buckling.

NASA Langley Research Center
Hampton, VA 23665-5225
January 21, 1992

References

1. Dow, Norris F.; and Hickman, William A.: *Design Charts for Flat Compression Panels Having Longitudinal Extruded Y-Section Stiffeners and Comparison With Panels Having Formed Z-Section Stiffeners.* NACA TN 1389, 1947.

2. Dow, Norris F.; and Hickman, William A.: *Comparison of the Structural Efficiency of Panels Having Straight-Web and Curved-Web Y-Section Stiffeners.* NACA TN 1787, 1949.

3. Anderson, Melvin S.; and Stroud, W. Jefferson: A General Panel Sizing Computer Code and Its Application to Composite Structural Panels. *AIAA J.*, vol. 17, no. 8, Aug. 1979, pp. 892–897.

4. Starnes, J. H., Jr.; Rhodes, M. D.; and Williams, J. G.: Effect of Impact Damage and Holes on the Compressive Strength of a Graphite/Epoxy Laminate. *Nondestructive Evaluation and Flaw Criticality for Composite Materials*, R. B. Pipes, ed., ASTM Spec. Tech. Publ. 696, c.1979, pp. 145–171.

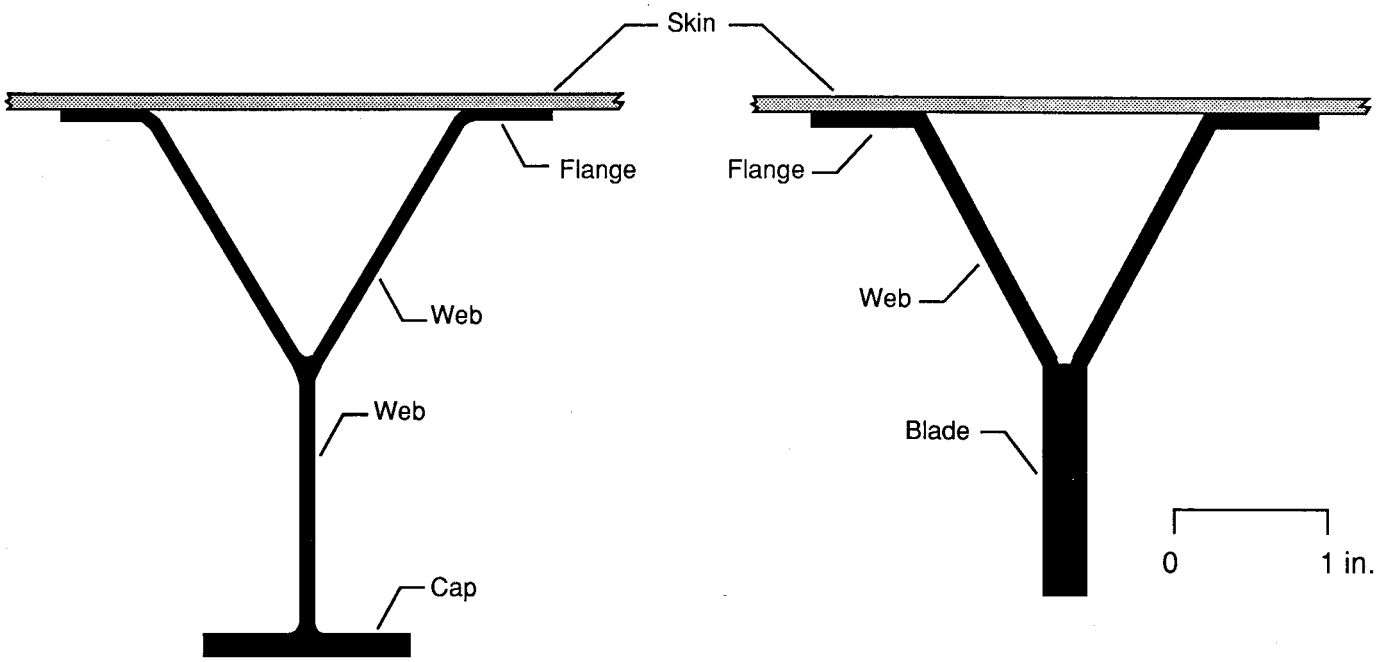

(a) Metal NACA Y-stiffener.

(b) Composite Y-stiffener.

Figure 1. Y-stiffener configurations.

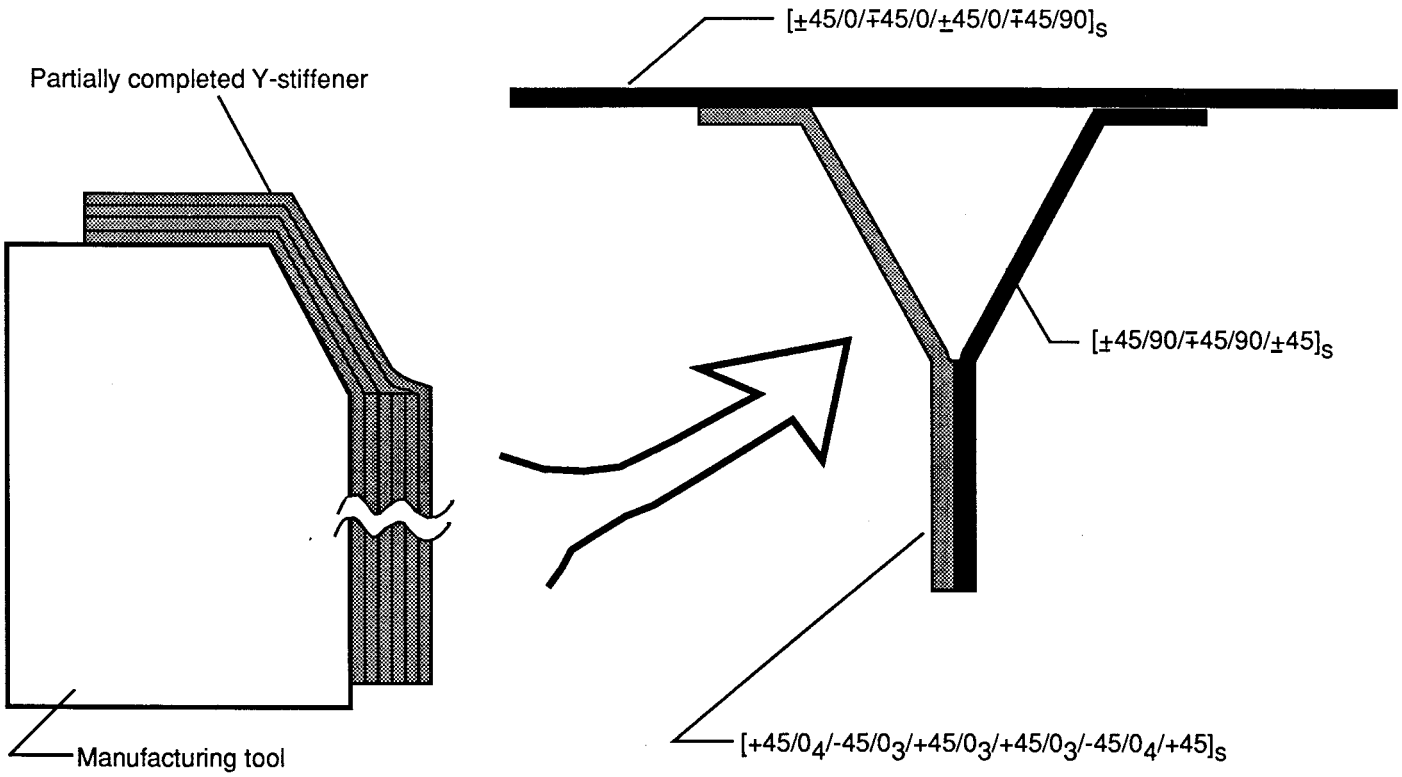

Figure 2. Fabrication of composite Y-stiffener element.

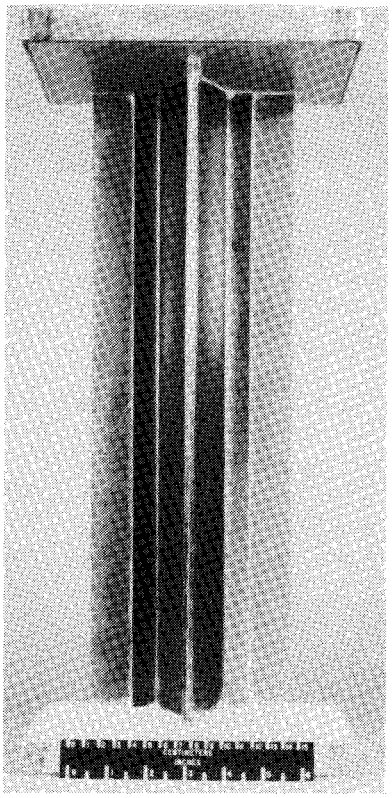

(a) Single-stiffener element specimen.

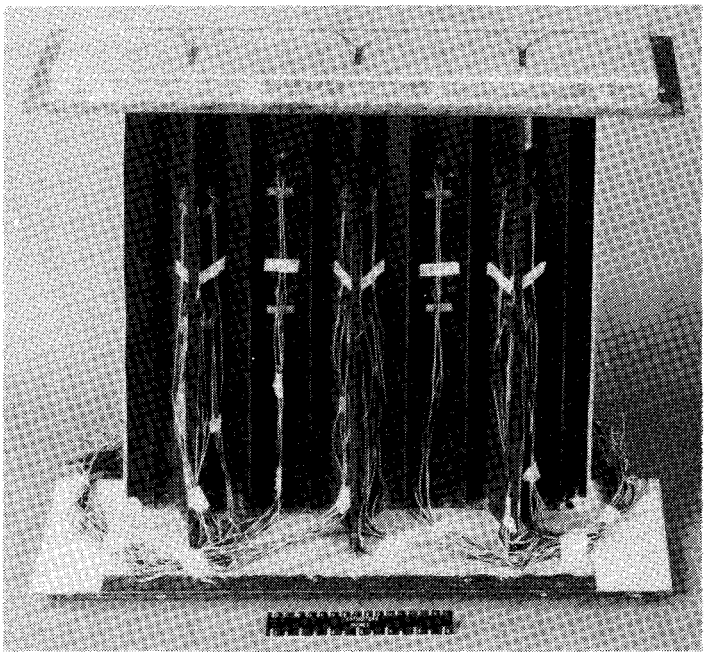

(b) Three-stiffener panel specimen.

L-90-12573

Figure 3. Y-stiffened specimens.

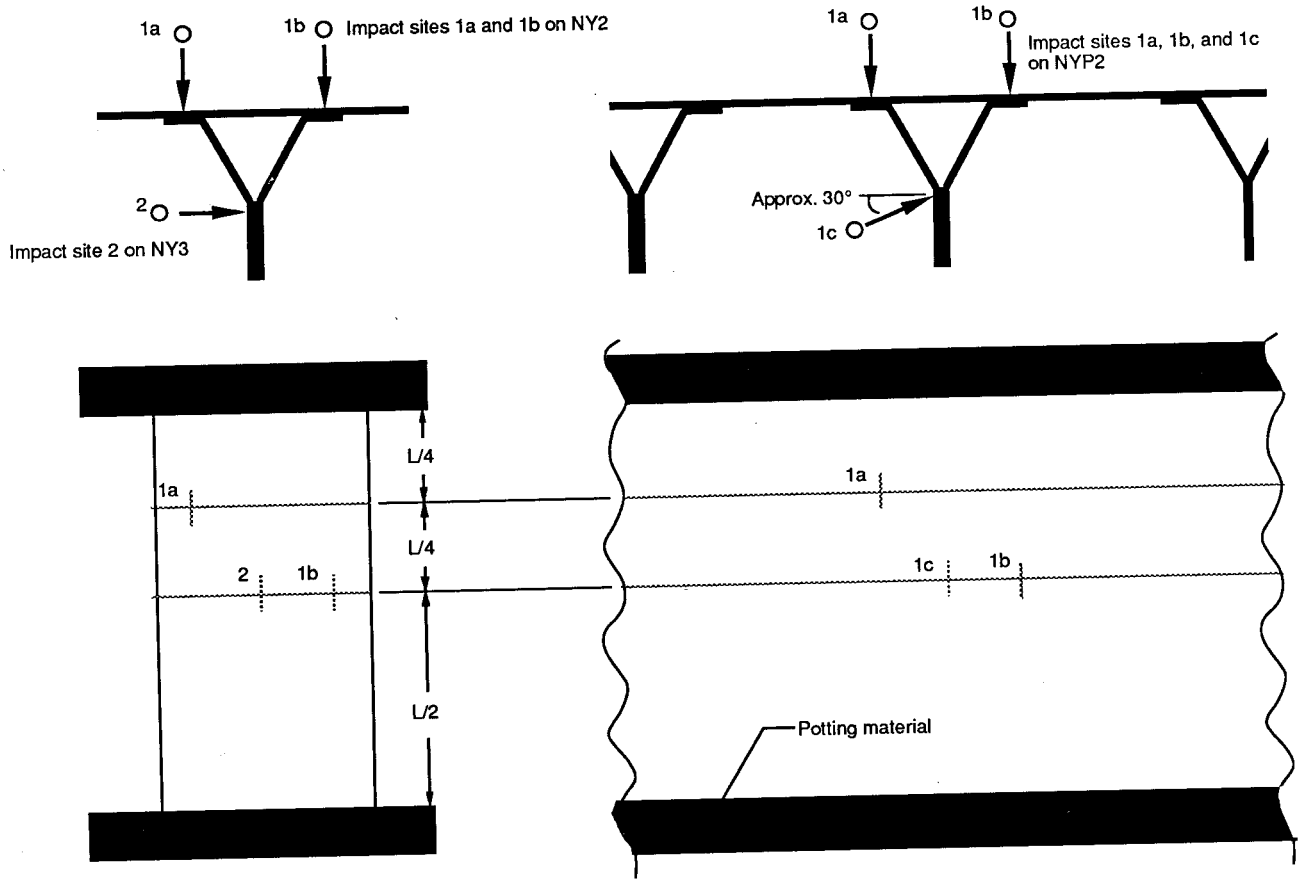

(a) Element specimens.

(b) Panel specimens.

Figure 4. Impact sites for Y-stiffened specimens.

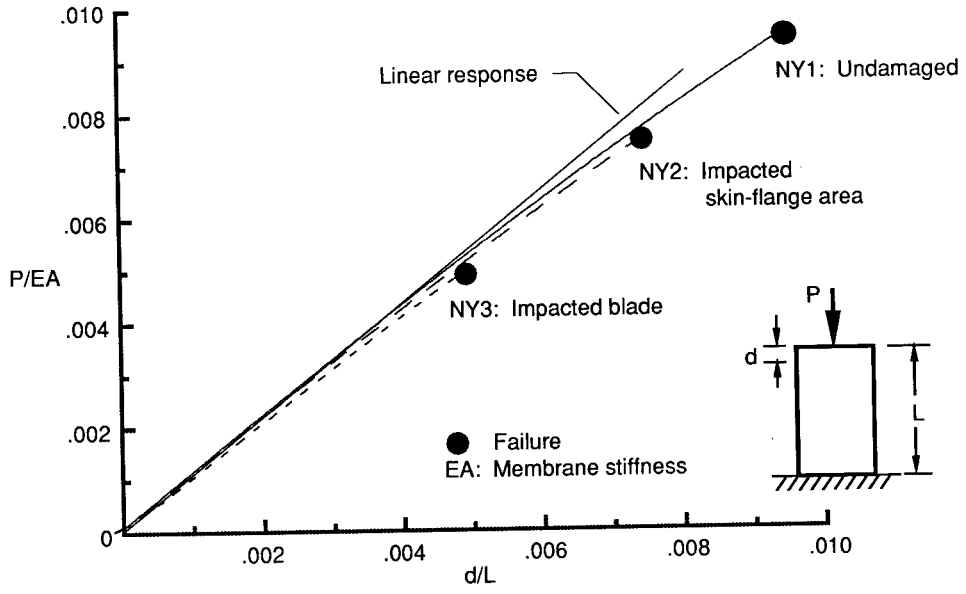

Figure 5. Normalized load versus end-shortening for Y-stiffened element specimens.

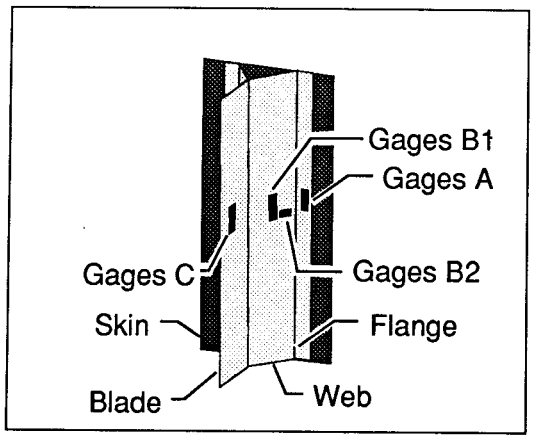

(a) Strain gage locations.

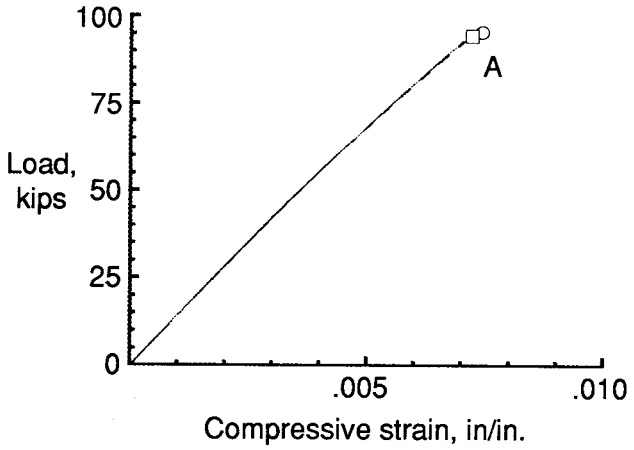

(b) Strain in skin and flange.

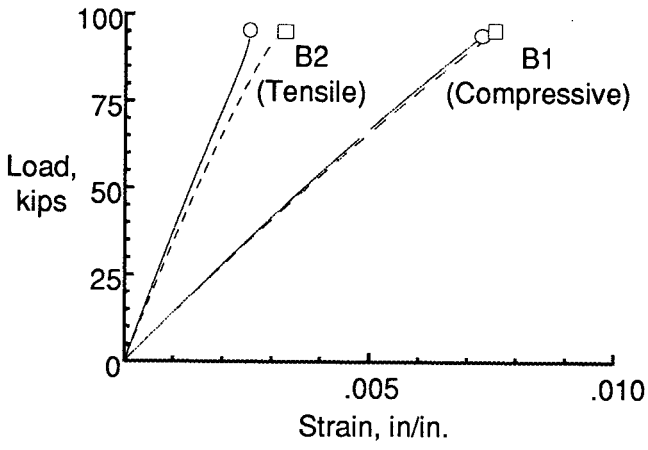

(c) Strain in web.

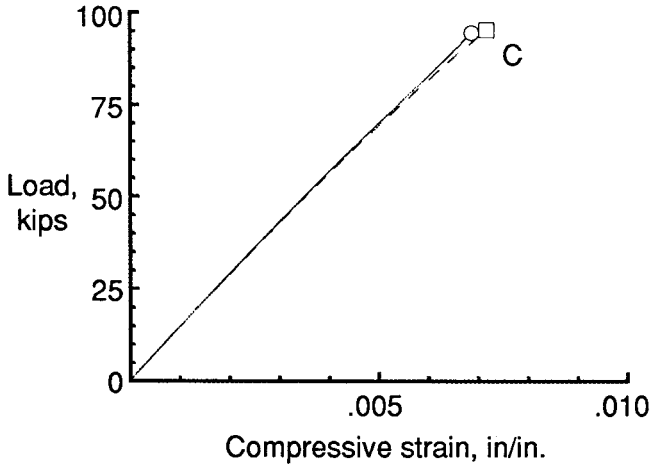

(d) Strain in blade.

Figure 6. Strain gage results for undamaged element specimen NY1 (square and circular symbols used to distinguish between individual gages).

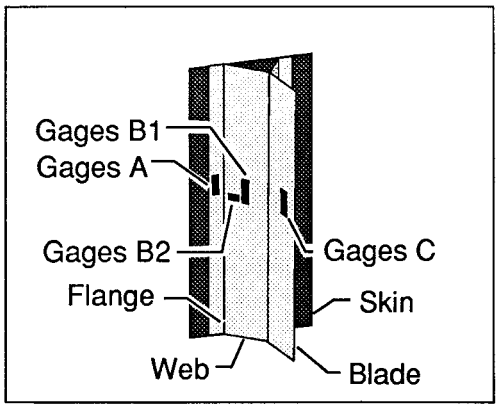

(a) Strain gage locations.

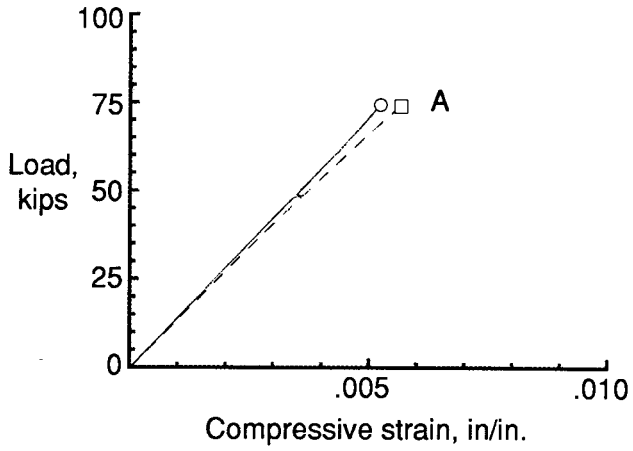

(b) Strain in skin and flange.

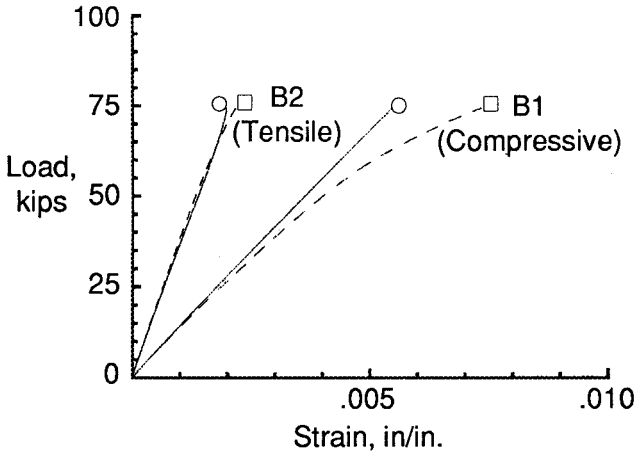

(c) Strain in web.

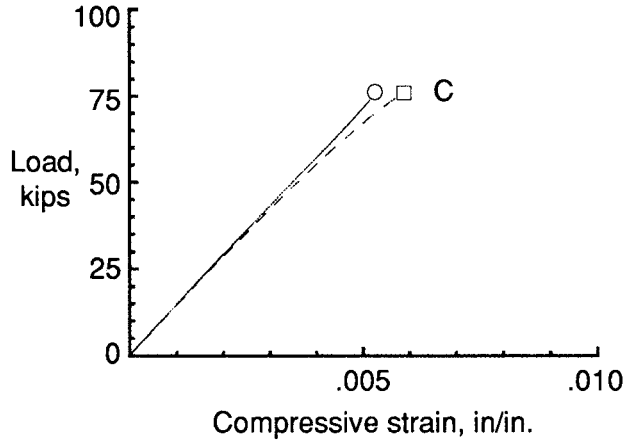

(d) Strain in blade.

Figure 7. Strain gage results for impact-damaged element specimen NY2 (square and circular symbols used to distinguish between individual gages).

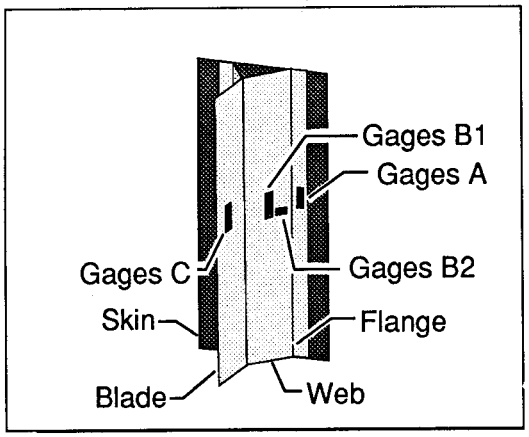

(a) Strain gage locations.

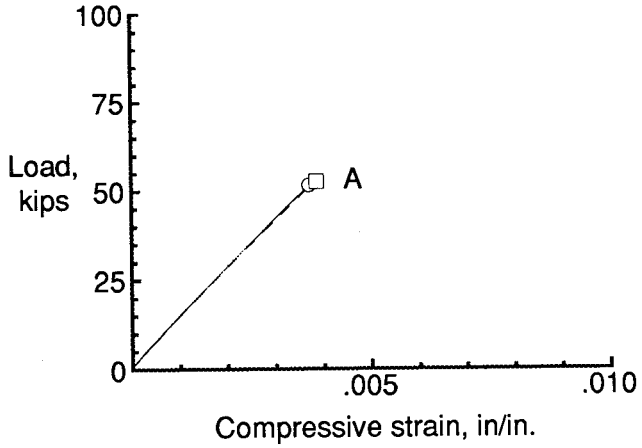

(b) Strain in skin and flange.

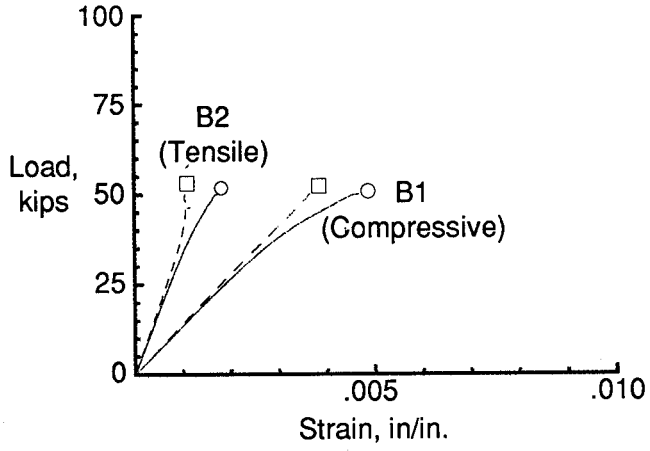

(c) Strain in web.

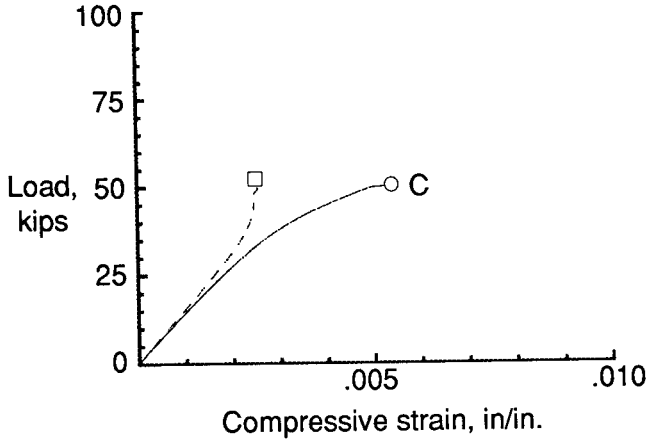

(d) Strain in blade.

Figure 8. Strain gage results for impact-damaged element specimen NY3 (square and circular symbols used to distinguish between individual gages).

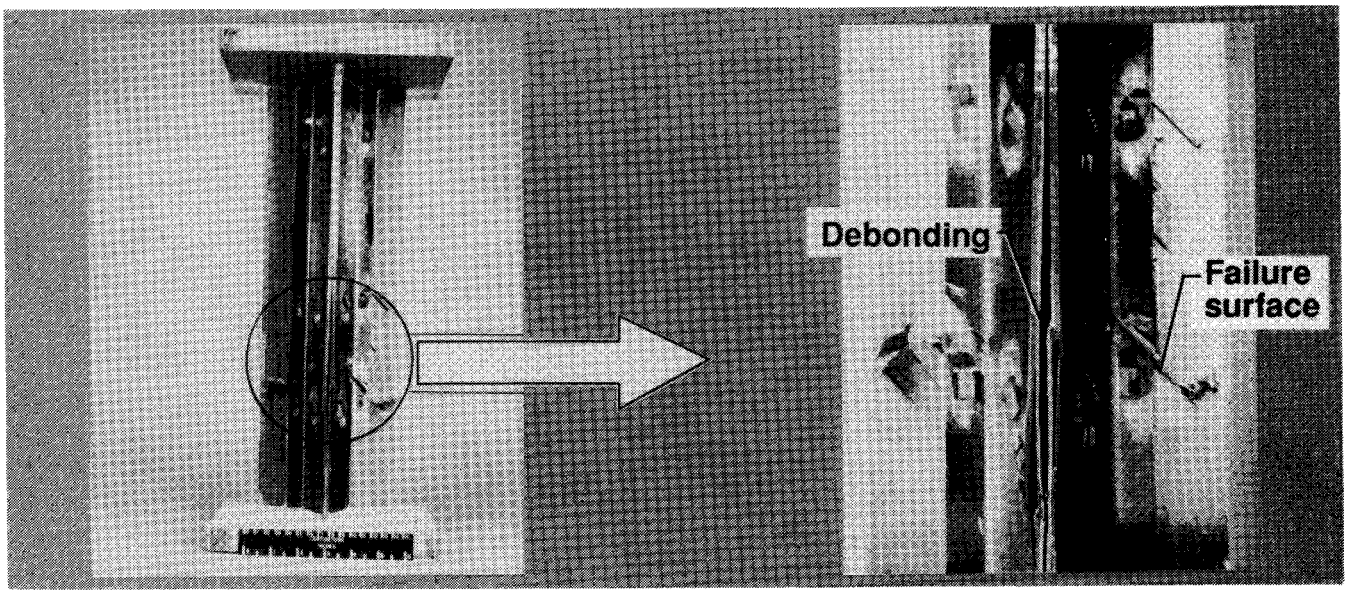

Failed element specimen

Failure region

L-90-12574

Figure 9. Typical failure of Y-stiffened element specimen.

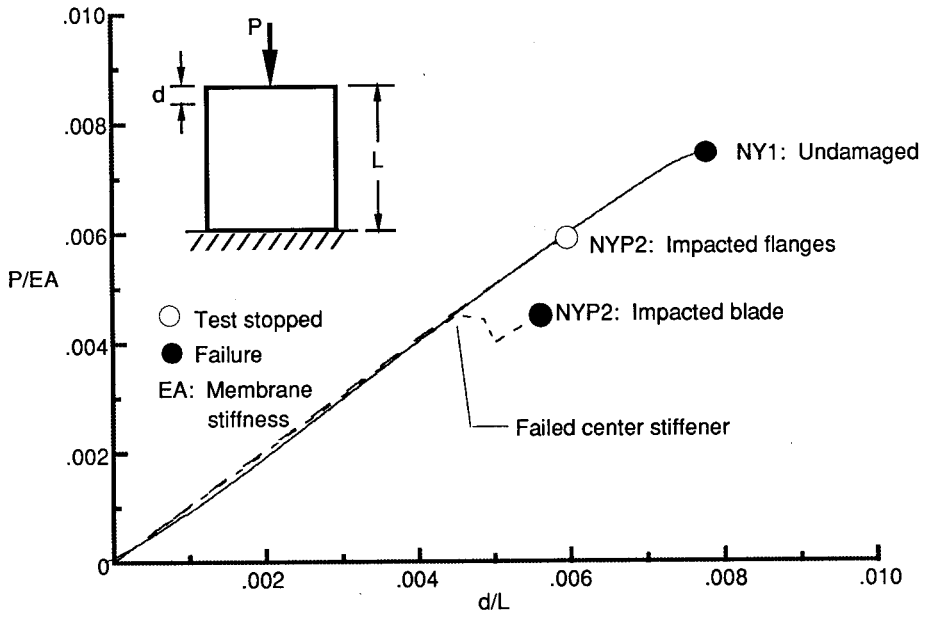

Figure 10. Normalized load versus end-shortening for Y-stiffened panel specimens.

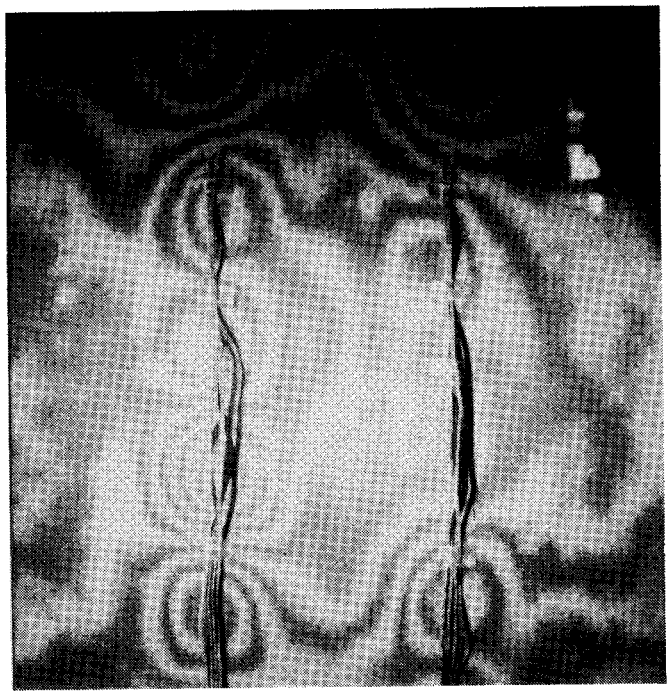

(a) Specimen NYP1; $P = 283$ kips ($P/P_{\max} = 0.992$).

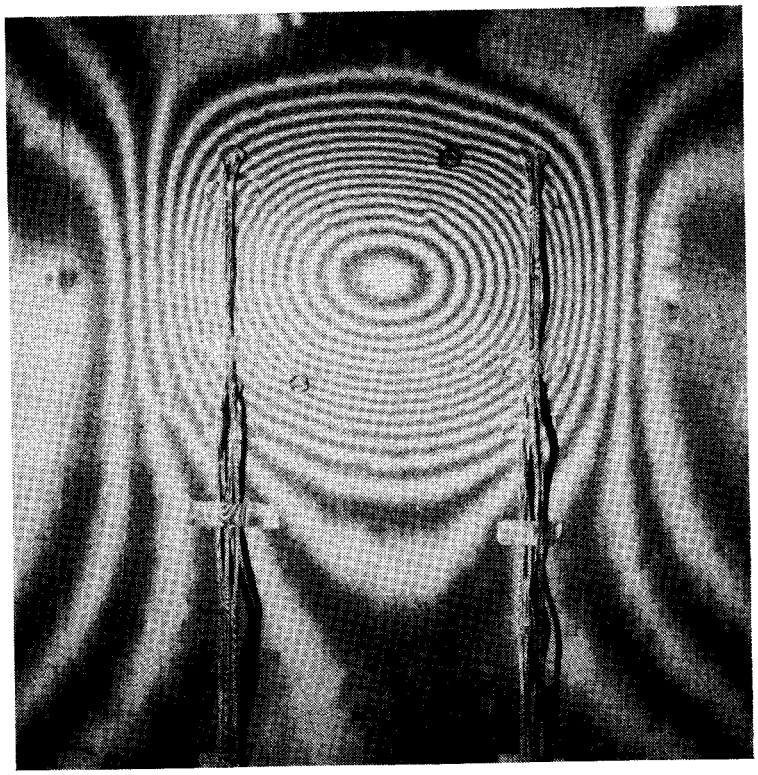

(b) Specimen NYP2; $P = 137$ kips ($P/P_{\max} = 0.998$).

Figure 11. Photographs of moiré fringe patterns for Y-stiffened panel specimens.

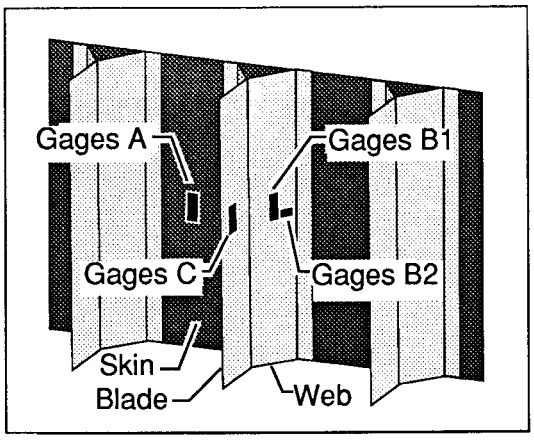

(a) Strain gage locations.

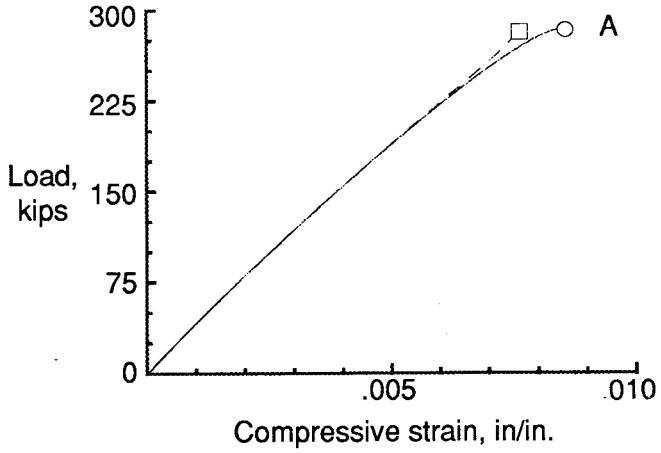

(b) Strain in skin.

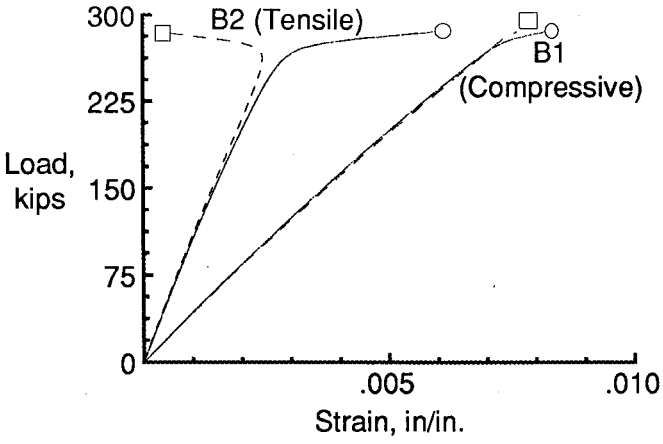

(c) Strain in web.

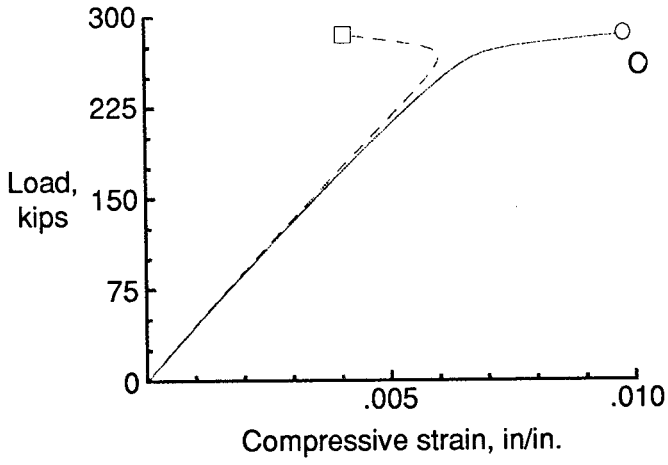

(d) Strain in blade.

Figure 12. Strain gage results for undamaged panel specimen NYP1 (square and circular symbols used to distinguish between individual gages).

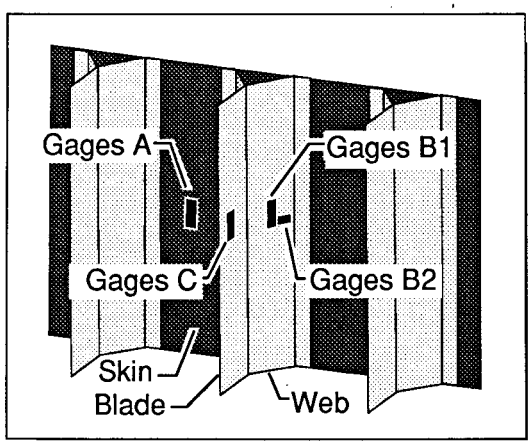

(a) Strain gage locations.

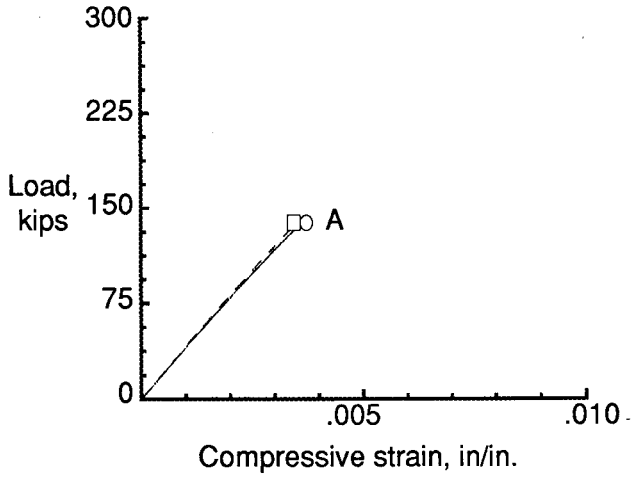

(b) Strain in skin.

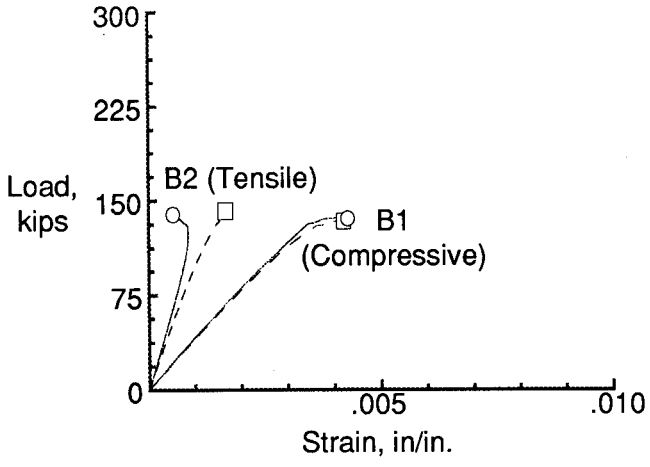

(c) Strain in web.

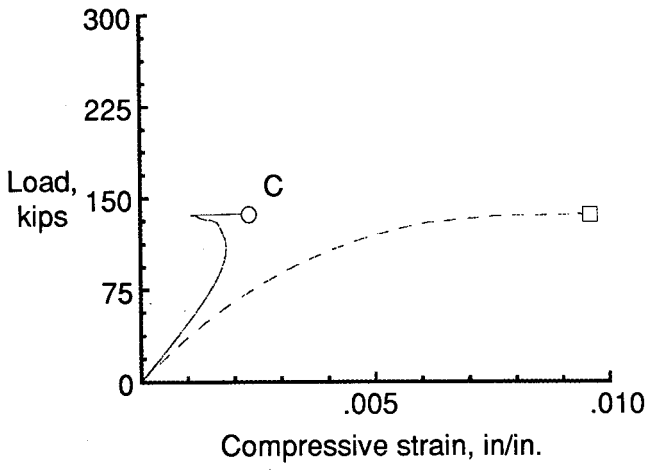

(d) Strain in blade.

Figure 13. Strain gage results for impact-damaged panel specimen NYP2 (square and circular symbols used to distinguish between individual gages).

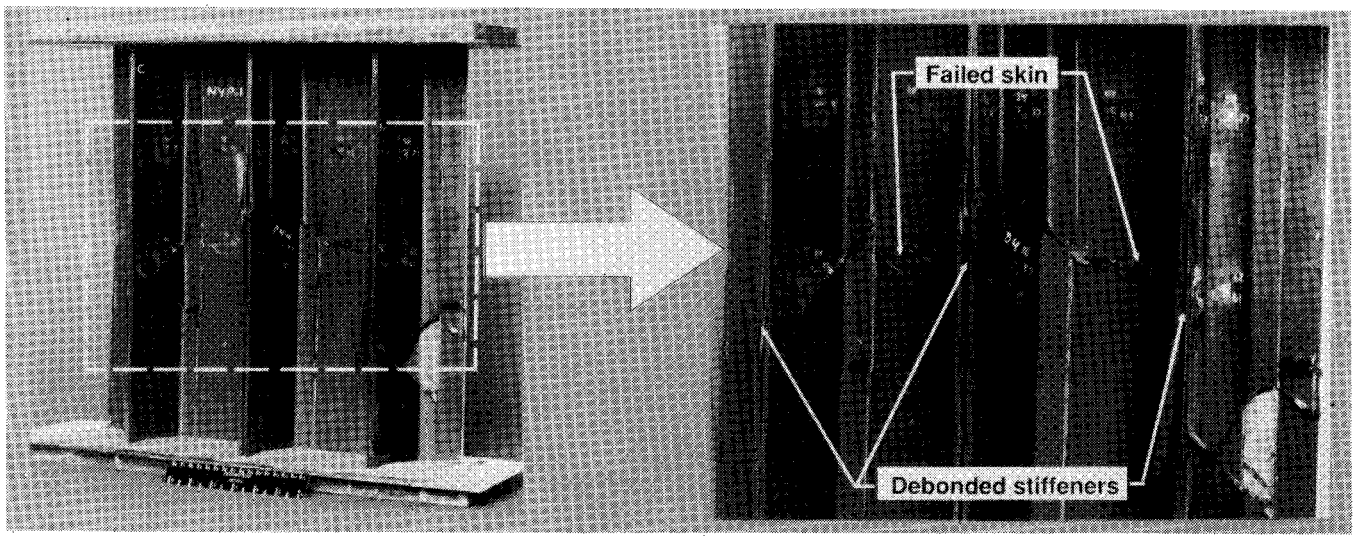

Failed panel specimen NYP1 Failure region

L-90-12575

Figure 14. Failure mode of Y-stiffened panel specimen NYP1.

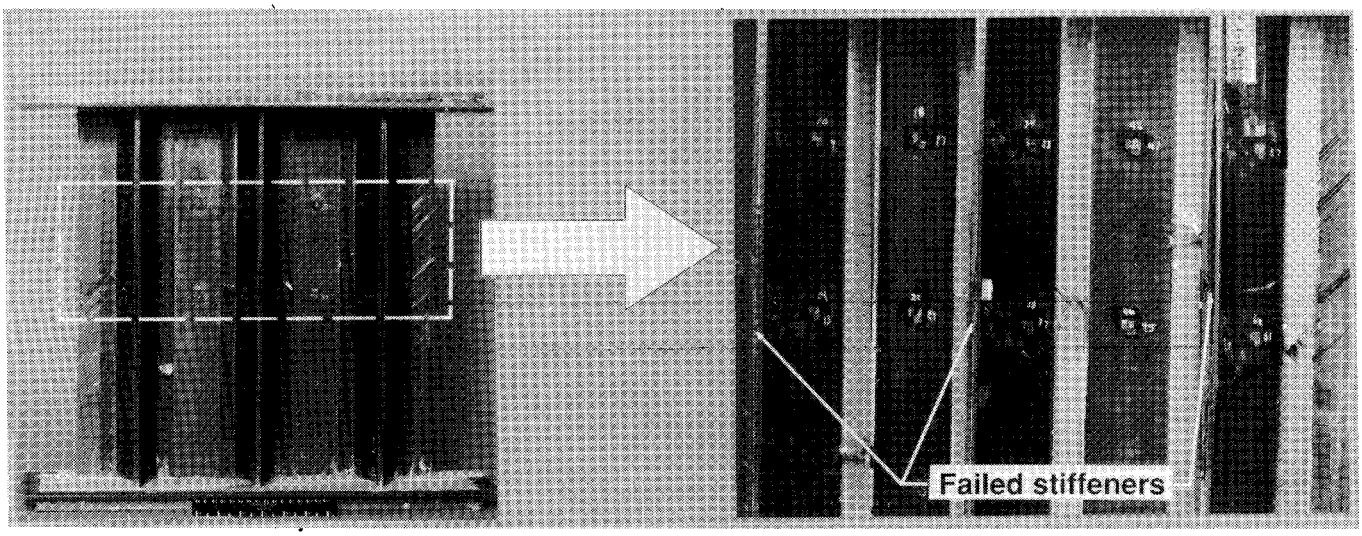

Failed panel specimen NYP2 Failure region

L-90-12576

Figure 15. Failure mode of Y-stiffened panel specimen NYP2.

REPORT DOCUMENTATION PAGE

Form Approved
OMB No. 0704-0188

1. AGENCY USE ONLY *(Leave blank)*	2. REPORT DATE	3. REPORT TYPE AND DATES COVERED
	April 1992	Technical Paper

4. TITLE AND SUBTITLE
Experimental Behavior of Graphite-Epoxy Y-Stiffened Specimens Loaded in Compression

5. FUNDING NUMBERS
WU 505-63-50-08

6. AUTHOR(S)
P. Daniel Sydow and Mark J. Shuart

7. PERFORMING ORGANIZATION NAME(S) AND ADDRESS(ES)
NASA Langley Research Center
Hampton, VA 23665-5225

8. PERFORMING ORGANIZATION REPORT NUMBER
L-16918

9. SPONSORING/MONITORING AGENCY NAME(S) AND ADDRESS(ES)
National Aeronautics and Space Administration
Washington, DC 20546-0001

10. SPONSORING/MONITORING AGENCY REPORT NUMBER
NASA TP-3171

11. SUPPLEMENTARY NOTES

12a. DISTRIBUTION/AVAILABILITY STATEMENT
Unclassified–Unlimited

Subject Category 39

12b. DISTRIBUTION CODE

13. ABSTRACT *(Maximum 200 words)*

An experimental investigation of the behavior of graphite-epoxy Y-stiffened specimens loaded in compression is presented. Experimental results are presented for element specimens with a single stiffener and for panel specimens with three stiffeners. Response and failure characteristics of the specimens are described. Effects of impact damage on structural response for both specimen configurations are also presented. Experimental results indicate that impact location may significantly affect the residual strength of the Y-stiffened specimens. The failure results indicate that the critical failure mode is buckling of the stiffener webs for Y-stiffened element specimens and buckling of the stiffener webs and the stiffener blades for the Y-stiffened panel specimens.

14. SUBJECT TERMS	15. NUMBER OF PAGES
Compression; Composite materials; Stiffened plates; Impact damage; Crippling; Failure	18
	16. PRICE CODE: A03

17. SECURITY CLASSIFICATION OF REPORT	18. SECURITY CLASSIFICATION OF THIS PAGE	19. SECURITY CLASSIFICATION OF ABSTRACT	20. LIMITATION OF ABSTRACT
Unclassified	Unclassified		